About the effect of two-phase flow formulations on shock waves in flash metastable expansions

Egoï Ortego

NICFD 2022
For Propulsion & Power

About the effect of two-phase flow formulations on shock waves in flash metastable expansions simulations

Egoi Ortego Sampedro
Mines Paris PSL
Centre d'Efficacité Energétique des Systèmes
egoi.ortego@minesparis.psl.eu
Palaiseau, France

ABSTRACT

Two-phase expanders are promising conversion machines that could help in increasing the energy efficiency of several systems such as heat-to-power plants, liquefaction processes or chillers. Expansion of two-phase flows is complex to model since the dynamics of the liquid-gas interactions depend on several factors. This work gives a preliminary insight on the effect of various formulations for liquid-gas interaction terms on the shock waves that may appear in over-expanded flash nozzles simulations. The case study is a water thrust nozzle from literature designed for geothermal energy conversion at inlet temperatures close to 150°C. The compared formulations differ mainly on the homogeneity assumptions regarding momentum and on the interface mass transfer term. The simulations results suggest that these assumptions have a fundamental effect on the flow behavior close to the outlet of the nozzle and in particular on the presence or not of the shock waves. This has meaningful consequences on the velocity profile in the nozzle.

Keywords: flash boiling, expansion nozzles, non-homokinetic, interfacial transfer

1. INTRODUCTION

The renewed interest in two-phase turbines in the last years can be explained by several factors. Some of them are the need for diversification of electricity production sources (by the use of waste-heat driven Organic Rankin Cycles for example), the reduction of electricity consumption of cold power production systems (especially in the context of natural refrigerants deployment), or the increase of computational capabilities for the design of two-phase components in the last 5 to 7 years that helps for the design of such machines.

However, flashing flows are highly driven by non-ideal phenomena and there is still no consensus on simulation methodology and assumptions that would lead to satisfactory results for the two-phase expanding flows modeling. This is in particular the case of the phase velocities homogeneity assumption. For example, considering the case of hot water flash expansion, Downar-Zapolski et al. (P.Downar-Zapolski, Z.Bilicki, L.Bolle, & J.Franco, 1996) considered no velocity difference between liquid and vapor whereas Liao & Dirk (Liao & Dirk, 2015) considered it because according to them it has great importance on the interfacial mass and heat transfer mechanisms. Besides, the velocities homogeneity assumption is very usual in the domain of two-phase expanding ejectors (Bodys, et al., 2021). However, knowing that vapor has a lower density than liquid, for a given pressure gradient, the acceleration observed by the vapor is higher. This results in higher velocities for vapor than for liquid during the expansion. This was observed by various studies (Elliott, 1982) (Sampedro, Breque, & Nemer, 2022). So velocities homogeneity assumption is likely to be incorrect. Nevertheless, the consequences of homogeneous and non-homogeneous assumptions need to be quantified.

This paper aims to analyze the effects of the velocities homogeneity assumption on the flow modeling results. In particular, the pressure and velocity profiles and the presence or not of a shock wave in simulations are analyzed. This is done on the case study of a hot water thrust nozzle tested by Ohta et al. (Ohta, Fuji, Akagawa, & Takenaka, 1993). The analysis of two-phase expansion nozzles presents the interest of being a relatively simple case of study that can also be considered as a real-life component used in particular as a stator in a low degree of reaction turbines. The experimental pressure profile data by Ohta et al. (Ohta, Fuji, Akagawa, & Takenaka, 1993) are used as a reference.

The computational fluid mechanics (CFD) model used in this paper is based on the general Euler-Euler description for two-phase flows. The interfacial mass transfer is modeled using two approaches to test the sensitivity of the simulation results to this aspect. Regarding the interface momentum coupling assumptions, two extreme situations were analyzed: the homogeneous and the non-homogeneous. The last was modeled using an interface friction formulation based on an interface drag coefficient from the literature. In addition, three supplementary values of the drag coefficient were tested to virtually observe the implications of this term in the flow behavior.

Then, the validity of the models is discussed based on the pressure profiles analysis. Besides, the paper gives a special insight into the literature models for sound velocity estimation. These models are used to analyze the CFD simulation results.

2. METHODS AND EQUATIONS

2.1. Models and definitions

The general formulation of conservation equations for a two-phase flow requires a phase-per-phase description i.e. an Euler-Euler formulation. In the literature dealing with flash nozzle flows, the general multiphase description is often reduced to simpler formulations. For further insight into these aspects, the reader is invited to read the very useful review maide by Yixiang & Dirk (Yixiang & Dirk, 2017) or the models' benchmark previously made by the author (Sampedro, Breque, & Nemer, 2022). In this paper, the general Euler-Euler formulation is adopted using the commercial software Ansys CFX. The detail of the equations is presented in a previous paper by the author (Sampedro, Breque, & Nemer, 2022). The CFX solver can handle, in an Euler-Euler formulation, all the assumptions to be tested on the coupling terms between phases. This is valid also for velocities homogeneity and non-homogeneity.

As a general remark for the rest of the article, since the term homogeneous is not specific enough from a semantic point of view, for clarity reasons regarding each assumption done on the coupling terms between the phases, the following definitions are adopted:

- Homokinetic: assumption of velocities equality between phases
- Homothermal: assumption of temperatures equality between phases

Regarding the mass transfer models, a substantial diversity in the interfacial transfer models exists as can be read in (Yixiang & Dirk, 2017). In the present, paper a thermal phase change model explored by the author (TABD model (Sampedro, Breque, & Nemer, 2022)) and the so-called Homogeneous Relaxation Model (HRM (P.Downar-Zapolski, Z.Bilicki, L.Bolle, & J.Franco, 1996)) are used. The motivation for using two mass transfer models is to separate the **effects** of mass and momentum interfacial transfer terms on the results.

For both models, heat transfer was assumed to occur between phases. Since the test case is the same that in the present paper, the reader is invited to read the complete configuration and calibration parameters for both models used by the author in previous work (Sampedro, Breque, & Nemer, 2022).

Regarding the momentum transfer, the liquid/vapor interfacial drag force is included for the general case. The standard drag coefficient has a value of $Cd = 0.44$. The homokinetic case is assumed to represent an extreme case where the interfacial forces would be enough high to avoid any difference in liquid and vapor velocities in any situation. To show the effect of the interfacial force on the phasic velocities, three additional values for Cd were tested (5, 50, and 500). A homokinetic case was also tested. The HRM mass transfer based cases associated with the non-homokinetic assumption were modeled using the same interfacial area density and characteristic length as TABD.

Regarding the properties of the fluids, the liquid properties (ρ, C_p, μ) were computed as a function of the temperature computed from the enthalpy resulting from the energy balance. This means that the liquid's meta-stable condition was computed by considering it in a temperature based saturation state and not in a pressure based saturation state. The vapor was supposed to be in pressure based saturated conditions i.e. its properties were a function of the static pressure. The liquid and vapor properties of water were computed from standard IAPWS IF97 tables available in Ansys CFX. The kwSST closure was used as turbulence model.

2.2. CFD simulation configuration

The control volume used for the simulations is presented in Figure 1. It represents the nozzle and an open volume at its outlet. This is a 3D domain maide by a partial revolution of 3 degrees. The inlet conditions are static pressure, static temperature, and liquid and vapor volume fractions. The outlet is defined as an opening with static pressure, and backflow temperature and volume fractions. The dimensions and boundary conditions values are given in section 3. The mesh was built by the same method and with the same characteristic sizes presented previously by the author (Sampedro, Breque, & Nemer, 2022). The mesh number per unit volume was similar in the nozzle than in the outlet volume. A mesh sensitivity was also presented in the cited work. The grid used here has 22500 elements.

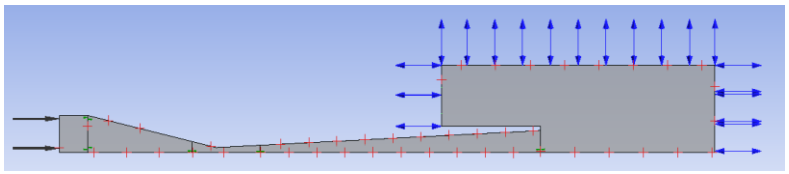

Figure 1: computational domain; black arrows : inlet; blue arrows : outlet

The commercial CFD code Ansys CFX 16.0 was used for CFD simulations. The CFX solver is a coupled solver using a pseudo-transient formulation; the coupled option was selected for volume fraction as well. A bounded second-order upwind scheme was selected for advection. Please refer to Ansys CFX (CFX, 2020) documentation for details on numerical resolution. A steady-state simulation was done. The physical time step was set to 1.10 - 5 s. This parameter acts like a relaxation coefficient. The simulation was supposed to be converged when the mass and energy imbalance was lower than 0.5%, the inlet mass flow rate was steady and the outlet velocity was steady; all residuals were in this situation lower than

1.10-5. The total energy formulation of the energy conservation equation was selected. The flow field was initialized at 0 vapor volume fraction, at inlet temperature and pressure, and at 0m/s velocity.

2.3. Speed of sound

The speed of sound is a parameter that helps in analyzing the flow. The two-phase flow speed of sound is not obvious to estimate since the wave propagation in a two-phase media is affected by several parameters. Among these, the following can be mentioned: interfacial mass transfer, heat and momentum transfers, and sound wave frequency (Staedtke, 2006). Depending on the intensity of the interfacial coupling terms, the effective speed of sound will differ from the ideal homokinetic homothermal case.

The following lines aim to give a summary of the approaches and concepts nowadays available to handle this question.

Staedtke presents the case of the homokinetic non-homothermal case where mass exchange between phases is considered. The resulting sound velocity is the following (Staedtke, 2006)(page 61):

$$a_{hke}^2 = \frac{1}{\frac{\alpha_g \rho}{\alpha_g^2 \rho_g} + \frac{\alpha_l \rho}{\alpha_l^2 \rho_l}} \tag{1}$$

This expression was also used by (White, 2020) to describe the so-called ‘’frozen homogeneous’’ situation. White explores as well the expression proposed by Brennen (Brennen, 2005) for homokinetic homothermal situation (White, 2020):

$$\frac{1}{\rho a_{Bren}^2} = \alpha_g g_g + \alpha_l g_l \tag{2}$$

The terms g_g and g_l depend on liquid and vapor phases state functions partial derivatives. Please refer to (White, 2020) or (Brennen, 2005) for the details.

For the non-homokinetic case, Wallis (Wallis, 1969) proposed an expression of sound velocity:

$$a_{Wallis}^2 = \frac{\alpha_g \rho_l + \alpha_l \rho_g}{\frac{\alpha_g \rho_l}{\alpha_g^2} + \frac{\alpha_l \rho_g}{\alpha_l^2}} \tag{3}$$

However, according to Staedtke (Staedtke, 2006), this expression leads to numerical instabilities in the computational codes using it. Staedtke presents the results of the work done by the Joint Research Center Ispra. He gives a particular insight into the virtual mass force that affects the speed of sound. This force represents the non-viscous interaction forces due to relative acceleration between phases and is associated with space and time derivatives of transfer terms. Brennen mentions them as the terms emerging from the averaging process in two-phase modeling (Brennen, 2005). The formulation of this force is based on the ‘’virtual mass’’ coefficient (k) in the work on Staedtke. The resulting sound velocity is the following (Staedtke, 2006):

$$a^2 = \frac{\alpha_g \rho_l + \alpha_l \rho_g}{\frac{\alpha_g \rho_l}{\alpha_g^2} + \frac{\alpha_l \rho_g}{\alpha_l^2}} \frac{1 + k \frac{\alpha_g \rho_g + \alpha_l \rho_l}{\alpha_g \rho_l + \alpha_l \rho_g}}{1 + k \frac{\rho^2}{\rho_g \rho_l}} - \alpha_g \alpha_l \rho_g \rho_l (u_g - u_l)^2 \frac{(\rho_l + k\rho)(\rho_g + k\rho)}{(\rho_g \rho_l + k\rho^2)^2} \tag{4}$$

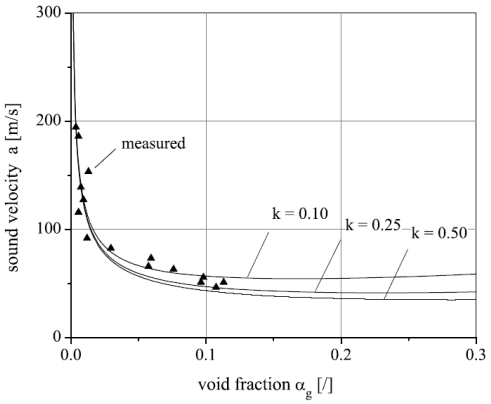

Figure 2: Sound velocity in water/steam media as a function of the void fraction; saturated conditions at pressure p = 1 bar (Staedtke, 2006)

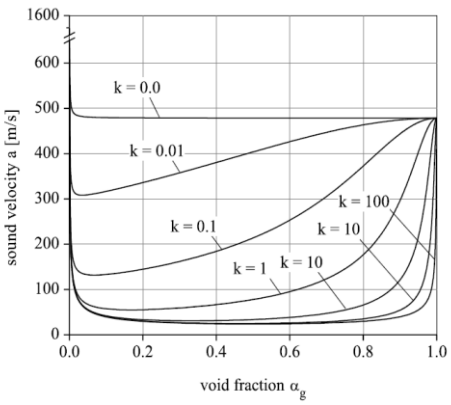

Figure 3: Two-phase sound velocity as a function of α; effect of the “virtual mass” coefficient, saturated water/steam at pressure p = 1 bar, equal phase velocities. (Staedtke, 2006)

The ‘’virtual mass’’ coefficient of k=0 represents a case with spatially separated phases where the momentum coupling is reduced to friction. If the friction term is small ($|u_g - u_l|/u < 0.1$), then the expression of ‘’a’’ is reduced to the one of

Wallis (eq 3). If the ''virtual mass'' coefficient k → ∞ then the flow is driven towards homokinetic conditions and the expression of "a" approaches "a_{hke}".

The ''virtual mass'' coefficient (k) was used by Staedtke as a calibration parameter for the two-phase flow computational method he presents in his book to estimate the sound velocity of water/steam flows. Staedtke mentions that the case where $0.25 \leq k \leq 0.5$ corresponds to dispersed droplets flows and fits well with experimental observations. Figure 2 presents an example where a coefficient of k=0.25 represents well the measurements. Figure 3 shows an extensive sensitivity analysis of the sound velocity in the entire range of void fraction (or vapor volume fraction) for the same media.

The sound velocity estimations will be used to analyze the simulation results presented below. In Ansys CFX, virtual mass modeling is not considered for two continuous phase's description (it can be for dispersed media). For that reason, the effect of parameter "k" will not be considered. Only reference cases will be used i.e. homokinetic non-homothermal (eq. 1), homokinetic homothermal (eq. 2), and non-homokinetic non-homothermal (eq. 3). Virtual mass effects are important to keep in mind from a theoretical point of view.

3. TEST CASE

In the early '90s, a Japanese team (Ohta, Fuji, Akagawa, & Takenaka, 1993) worked on waste heat recovery by impulse turbines using phase change nozzles. Two nozzle geometries were tested. The first was called the B nozzle which is a fairly simple nozzle. It was extensively studied for a wide outlet pressure range. The authors measured mass flow rate, efficiency, and pressure profiles. The efficiency was obtained thanks to thrust measurements. The dimensions and the operating conditions are shown in Figure 4 and Table 1 respectively.

Note that the mass flow in Table 1 does not depend on the outlet pressure; that means that the nozzle operates in critical conditions. The static pressure taps diameter was 0.6mm. The uncertainty on the pressure measurement was +/-1%.

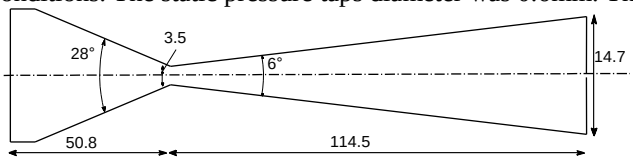

Figure 4 : Ohta B nozzle (Ohta, Fuji, Akagawa, & Takenaka, 1993)

Table 1 : Ohta B nozzle operating points (Ohta, Fuji, Akagawa, & Takenaka, 1993)

$T_{in}(°C)$	$P_{in}(kPa)$	$SC(K)$	$P_{out}(kPa)$	$\dot{m}(g/s)$
148	470	1,5	18/45/73/100	122
137,5	470	12	16/43/70/100	156

4. SIMULATION RESULTS

4.1. Pressure profiles

The pressure profiles will help in defining which assumption leads to the more reliable results. Pressure profiles obtained with TABD and HRM models are presented respectively in Figure 5 and Figure 6. Each line represents a different assumption on the interfacial momentum transfer term. The 0mm position corresponds to the throat position.

It appears that the main difference between TABD and HRM models occurs just after the throat. TABD gives pressures closer to experiments; however, the difference between models is not significant.

Regarding the assumptions on momentum transfer intensity, the difference between models appears in particular close to the nozzle outlet. The effect of this series of assumptions on the difference to experiments is also particularly visible close to the nozzle outlet. The homokinetic case presents a pressure profile characteristic of a shock wave i.e. a sudden static pressure increase. This is confirmed by velocity profiles as will be presented in section 4.2. However, for the lowest value of Cd, there is no shock wave and the pressure profile is very close to the measured one.

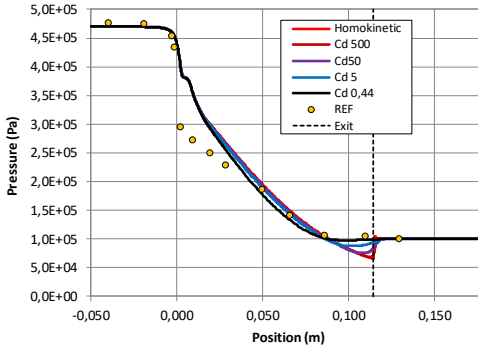

Figure 5: pressure profiles; simulation vs experiments ; TABD model

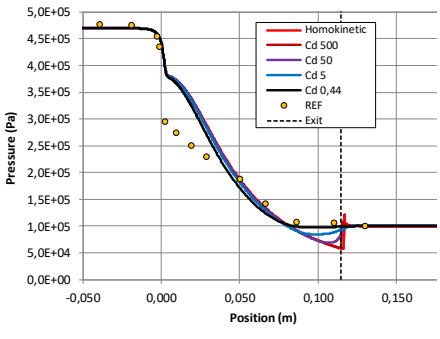

Figure 6: pressure profiles; simulation vs experiments ; HRM model

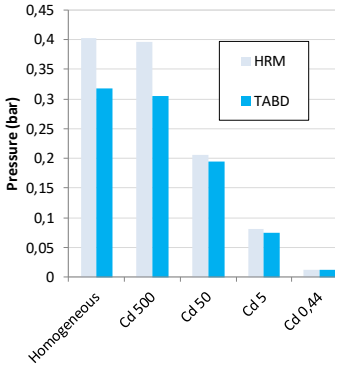

Figure 7: pressures absolute discrepancies for last pressure tap

The pressure tap located at 4mm before the outlet is of particular interest. At this location, the static pressure value obtained with the homokinetic assumption is lower than in reality. The absolute discrepancy to the experimental value is presented in Figure 7. The discrepancy increases with Cd. For the nominal Cd, the discrepancy is close to 0.01bar. For the homokinetic case, it is close to 0.3bar for TABD and 0.4bar for HRM.

4.2. Velocities

Figure 8 shows the liquid and vapor velocities obtained with the TABD model. The velocity difference between vapor and liquid reduces with increasing value of Cd as expected. However, getting the same velocity would require increasing a lot the value of Cd. Also, with the increasing value of Cd, the velocities of both phases get closer to the homokinetic case.

The homokinetic case shows a shock wave close to the nozzle outlet whereas the case with Cd=0.44 doesn't. The values computed for the sound velocity for the different models presented in section 2.3 are given in Figure 9. The figure gives also the values of the average mixture velocity before and after the nozzle outlet (respectively "av ex-4mm" and "av final"). The sound velocity models based on homokinetic assumption give low values of the speed of sound whereas the non-homokinetic model gives a high value (close to the vapor phase sound velocity).

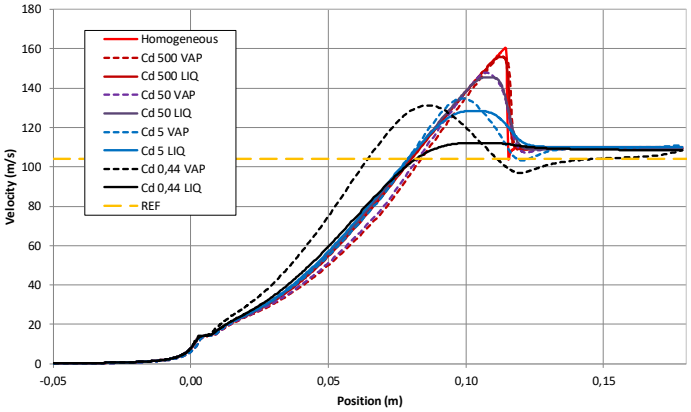

Figure 8: vapour and liquid velocities for TABD

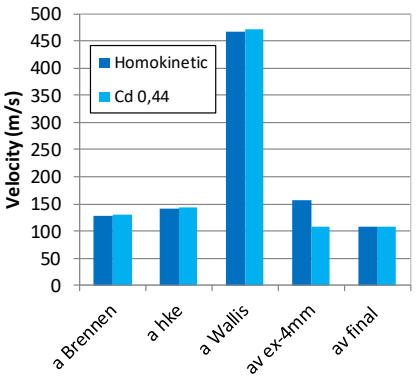

Figure 9: sound velocities and average velocities before and after outlet; TABD

For the homokinetic simulation, it appears that at some point, if the mixture velocity exceeds sound velocity, a shock wave may occur leading to a sudden increase in static pressure and a rapid drop of the velocity. It seems that the homokinetic assumption in the CFD simulation and its consequences on the sound velocity were modeled in coherence with literature models for homokinetic sound velocity i.e. $a_{Brennen}$ and a_{hke}.

For the case with Cd=0.44, the mixture average velocity remains always below all the sound velocities computed. Besides, no shock wave was observed for this CFD simulation. To explain this, two hypotheses may be possible:

- The sound velocity in the non-homokinetic case is very high as suggested by the Wallis model. In this case, the momentum coupling between phases is weak and the CFD simulation represents it relatively well. This suggests that frictional and non-friction coupling terms are small and could be reduced to frictional only (at least close to the nozzle outlet in the given conditions). Please note that the Wallis model is close to the model presented by Staedtke in the case of dispersed flow (small value of "k") which corresponds to the high void fraction situation in the last third of the nozzle.
- The non-homokinetic case creates so much friction that the total enthalpy of the flow is highly degraded leading to moderate maximal velocity. This velocity is thus never higher than any sound velocity.

The last hypothesis seems to the author not probable since in the last part of the expansion, where the maximum velocities are reached, the average vapor volume fraction is very high (0.99) and the mixture density is very low (6kg/m^3). Furthermore, given the moderate length, such energy losses seem unlikely. However, this needs to be verified in the future.

5. CONCLUSIONS AND FUTURE WORKS

The simulation based on the homokinetic assumption produces a two-phase mixture shock wave close to the nozzle outlet. The presence of this shock is coherent with the sound velocity models from the so-assumed homokinetic mixture theory. The non-homokinetic case doesn't show any shock wave; that seems coherent with the non-homokinetic sound velocity models.

From the comparative analysis made on the static pressure profiles, it can be concluded that whatever the mass transfer model is, the homokinetic model provides unrealistic results at high velocity. The non-homokinetic model provides results in accordance with the measurements. It can be concluded that the homokinetic assumption implies very important interface momentum coupling that provides erroneous simulated flow velocities and pressures. This has particularly remarkable effects when the homokinetic mixture velocity attains homokinetic sound velocity. It would be useful to consolidate the results on pressure profiles by measuring a larger number of pressure points close to the nozzle outlet.

Also, the interfacial momentum transfer modeling needs to make assumptions on the interfacial area density. For the present work, the parameters used to set it were defined using the TABD model. And no extended analysis of the correctness of the drag coefficient value was discussed. It would be useful to analyze it further.

Finally, according to the Wallis model, the sound velocity in the non-homokinetic case is very high, close to pure vapor sound velocity. This is coherent with the model by Staedtke. However, these are theoretical models, and experimental measurement of sound velocity in mixtures, in particular at vapor volume fractions higher than 0.7, would be extremely useful for phase-changing expansions study. Besides, it seems that the momentum coupling between phases was weak in reality as suggested by Staedtke for mist flows. For that reason, including the non-frictional momentum transfer terms was not problematic for the presented case. However, for mixtures with lower vapor/liquid density ratios, this may be no more valid and thus these terms could require further research.

REFERENCES

Bodys, J., Smolka, J., Palacz, M., Haida, M., Banasiak, K., & Nowak, A. J. (2021). Experimental and numerical study on the R744 ejector with a suction nozzle bypass. *Applied Thermal Engineering, 194*.

Brennen, C. E. (2005). *Fundamentals of Multiphase Flows.* Cambridge University Press.

CFX, A. (2020). *V20 User's Guide.*

Elliott, D. G. (1982). *Theory and Tests of Two-Phase Turbines.* Pasadena: Jet Propulsion Laboratory.

Liao, Y., & Dirk, L. (2015). 3D CFD simulation of flashing flows in a converging-diverging nozzle. *Nuclear Engineering Design*, 149-163.

Ohta, J. (1993). Performance and flow characteristics of nozzles for initially subcooled hot water (influence of turbulence and decompression rate). *International Journal of Multiphasse Flow, 19*(1), 125-136.

Ohta, J., Fuji, T., Akagawa, K., & Takenaka, N. (1993). Performance and flow characteristics of nozzles for initially subcooled hot water (influence of turbulence and decompression rate). *International Journal of Multiphasse Flow, 19*(1), 125-136.

P.Downar-Zapolski, Z.Bilicki, L.Bolle, & J.Franco. (1996). The non-equilibrium relaxation model for one-dimensional flashing liquid flow. *International Journal of Multiphase Flow, 22*, 473-483.

Sampedro, E. O., Breque, F., & Nemer, M. (2022). Two-phase nozzles performances CFD modeling for low-grade heat to power generation: Mass transfer models assessment and a novel transitional formulation,. *hermal Science and Engineering Progress*.

Staedtke, H. (2006). *Gasdynamic Aspects of Two-Phase Flow.* Weinheim: WILEY-VCH.

Wallis, G. B. (1969). *One-dimensional Two-phase Flow.* New York: McGraw-Hill.

White, M. (2020). Investigating the validity of the fundamental derivative in the equilibrium and non- equilibrium two-phase expansion of MM. *NICFD 2020.* Delft.

Yazdani, M., Radcliff, T. D., Alahyari, A. A., & Farzad, M. (2014). Numerical Modeling and Validation so Supersonic Two-Phase Flow of CO2 in Converging-Diverging Nozzles. *Journal of Fluid Engineering, 136*.

Yixiang, L., & Dirk, L. (2017). Computational modeling of flash boiling flows, a literature survey. *International Journal of Heat and Mass Transfer*, 246-265.

NOMENCLATURE

Roman symbols

a	Sound velocity (m/s)
C_d	Drag coefficient
C_p	Specific heat capacity at constant pressure (J/kg/K)
$\dot{m}$	Mass flow rate (kg/s)
k	Virtual mass coefficient
P	Pressure (Pa)
u	Velocity (m/s)
T	Temperature (K)

Greek symbols

α	Volume fraction
μ	Dynamic viscosity (Pa.s)
ρ	Density (kg/m^3)

Sub- / super-scripts

g	Gas or vapor
in	Inlet property
l	Liquid

Acronyms

CFD	Computational Fluid Mecanics
HRM	Homogeneous Relaxation Model
TABD	Thermal bubble-to-droplet